# An Optimized Polarization Model for Anode-Supported Solid Oxide Fuel Cells

K. Daneshvar[1*], M. Baghban Yousefkhani[2], H. Ghadamian[2], B. C. Rincon Troconis[1], G. Dotelli[3], M. Santarelli[4]

*[1]University of Texas at San Antonio, USA*
*Department of Mechanical Engineering*

*[2]Materials and Energy Research Center (MERC), Tehran, Iran*
*Department of Energy*

*[3]Politecnico di Milano, Italy*
*Department of Chemistry, Materials and Chemical Engineering "GIULIO NATTA"*

*[4]Politecnico di Torino, Italy*
*Department of Energy*

[*] Corresponding author: Keyvan Daneshvar
  Email address: keyvan.daneshvar@utsa.edu

## Abstract

A polarization model of an anode-supported Solid Oxide Fuel Cells (SOFCs) has been developed considering activation overpotential (Butler-Volmer equation), ohmic resistance, and concentration overpotential. In this work, the assembly of  Ni-YSZ / YSZ / LSM-YSZ as an anode, electrolyte, and cathode, respectively, was considered. An optimization process was also performed in order to verify the accuracy of the polarization model. Three optimum outputs obtained were cell voltage of 0.57 V, current density of 5620 A/m$^2$, and power density of 3205 W/m$^2$. The model has been tested against another modeling approach and experimental data. It was found that the results of our model compare well with the outcomes of another model. The model validation using literature experimental data was also satisfactory and acceptable. Finally, a parametric analysis has been carried out to highlight a number of parameters, which are most relevant in the overall cell performance as measured by polarization curve. In particular, the following parameters were accounted for in this analytical study: exchange current densities in anode and cathode ($j_{0a}$ and $j_{0c}$), leakage current density ($j_{Leak}$), and temperature (T).

*Keywords: SOFCs, Polarization Modeling, Optimization Process, Model Validation, Parametric Analysis.*

## 1. Introduction

Fuel cell is an emerging technology that is, to a great extent, promising for the achievement of higher energy efficiency and lower environmental load. In order to meet the requirements of the Kyoto Protocol, fuel cell was considered as an emerging technology [1-2]. SOFCs is one of the high-temperature fuel cells, which convert chemical energy of a fuel to electrical power through electrochemical reactions at high temperatures. These cells have high efficiency, fuel diversity, and lower air pollution potentials. In addition, they can be installed in combined cycle

plants to increase the efficiency level and lower the environmental pollution [3-5]. As result of its operation at high temperatures, SOFCs is often used in power plants and in heavy machineries [6-8].

Considerable research studies have been done on SOFCs in the last two decades [9-12]. Research in this field, including computational modeling, expanded the benefits and reduced the disadvantages, playing an important role in the affirmation of this technology as a viable energy alternative. In general, simulation and modeling are techniques being used since not long ago; however, their application has made a great contribution to scientific and industrial progresses, solving many un-known problems for mankind. Hence, mathematical problem solving techniques have been developed to bring the constructed models to an optimal condition. A summary of the most important findings is found below.

Liu et al. [13] studied anode-supported SOFCs by using Star-CD software, in order to measure the performance analysis parameters, including current density, fuel density, and rate of fuel consumption. Results from this work showed that power density is increased as the fuel consumption is decreased. In addition, the performance of fuel cell was shown to be improved by increasing the current discharge rate. Yakab et al. [14] studied some properties of SOFCs including fuel density, distribution of temperature, and density by using simple electrochemical models within specific mode. Chan et al. [15] offered a 1D model of SOFCs and observed only two types of electrodes for determining diffusion by using Fick's law. Within this model, the assumed temperature, the exchange current density, and the reactants density were fixed. It is important to highlight that the two last parameters are strongly dependent on temperature. Petruzzi et al. [16] investigated a thermo-electric model of SOFCs; the main disadvantages of their study was neglecting the concentration loss and applying the Tafel equation for modeling the activation loss. Autisser et al. [17] calculated the rate of reactions, the distribution of current density, gas current, temperature of the cell, and fuel density by developing infrastructures of fluent software. Zhu et al. [18] established a parametric model for anode-supported SOFCs to explain various polarizations, cell voltage, and power density as a function of current density based on measurements made on cell materials and components. In the research done by Shen et al. [19], a polarization model considering activation and ohmic polarization for SOFCs with a bi-layer electrolyte is presented. Also, the energy conservation equation is used to integrate the electronic conductivity with the local oxygen partial pressure. Based on their outputs, the Open Circuit Voltage (OCV) improves by increasing the cathode exchange current density. In addition, the leakage current density under OCV was found to be unrelated to the cathode exchange current density.

In order to improve the performance of the electrochemical cell by lowering the concentration polarization, Shimada et al. [20] developed a porous microstructure control technique to achieve high power density in Planer SOFCs. Designing a high porosity Ni-YSZ anode increased the power density from 1.95 to 3.09 Wcm$^{-2}$ at 800 °C using humidified H$_2$ fuel. As a key result of this study, porosity and pore size distribution in the electrodes were found to be essential to obtain a high performance electrochemical cell. The anode-cathode supported SOFCs (ACSC) was designed by Su et al. [21] to decrease the concentration and ohmic polarization that exist in the typical design of SOFCs. By using mathematical modeling, the results showed that the ACSC design improved the oxygen concentration distribution and the electric potential distribution in comparison with the anode-supported SOFCs (ASC).

As a summary, different research studies have already been performed using modeling tools to analyze both the polarization losses and their minimization process. Considering the

investigation of the previous studies and the gaps currently existent in the literature, one of the essential goals of this research is to identify a number of parameters, which are most relevant in the overall cell performance by carrying out a parametric analysis. For this purpose, a polarization model of an anode-supported SOFCs has been presented considering total losses including: activation, ohmic, and concentration overpotential. Then, an optimization process was performed to verify the accuracy of the polarization model. The model has been sucessfully tested against another modeling approach and experimental data. The following parameters were considered for the metioned parametric study: exchange current densities in anode and cathode ($j_{0a}$ and $j_{0c}$), leakage current density ($j_{Leak}$), and temperature of the cell (T).

## 2. Development of the polarization model

SOFCs is characterized by a solid oxide electrolyte that transports oxygen anions from the cathode to the anode: the most used material is the Yttria-Stabilized Zirconia (YSZ). The electrodes for SOFCs are made with solid oxides: the anode, where the electrochemical oxidation of hydrogen occurs, is a cermet made out of nickel mixed with YSZ (Ni-YSZ), while the cathode, where oxygen reduction takes place, is a composite of Lanthanum Strontium Manganite (LSM) and YSZ (LSM-YSZ). These materials were chosen to be used in our model. SOFCs could have different geometries, but laboratory scale experiments usually adopt anode-supported button cell geometry, which is the one chosen for our research study. This geometry was selected because the anode is the thickest and strongest layer placed on the bottom of the cell, providing mechanical support to the cell [22-25].

The polarization model uses the Butler-Volmer equation, the Ohm's law, and the Fick's law for description of the activation, ohmic, and concentration over-potentials, respectively. Taking into account all the over-potentials effecting SOFCs, the cell effective potential is given by:

$$V_{cell} = E_{cell} - (\eta_{act} + \eta_{ohm} + \eta_{conc} + V_{Leak}) \tag{1}$$

Where $E_{cell}$ (V) is the equilibrium voltage of the cell, $\eta_{act}$ (V) is the activation over-potential, $\eta_{ohm}$ (V) is the ohmic over-potential, $\eta_{conc}$ (V) is the concentration over-potential, and $V_{Leak}$ represents the voltage loss related to leakage.

There are several types of mathematical problem-solving techniques among which general linear and non-linear techniques can be mentioned. Usually, technical engineering problems are dynamic and non-linear and their solution is done by non-linear techniques. Eq. (2) shows the general form of a mathematical model [26]:

$$\begin{cases} Min\ F(x) \quad OR \quad Max\ F(x)\ [Objective\ Function] \\ \quad Sub.\ g(x) \geq 0 \quad OR \quad \leq 0\ [Cons.] \\ \quad\quad\quad X \geq 0 \end{cases} \tag{2}$$

In terms of the software used for this research, there are many software related to mathematical problem-solving methods among which Matlab is very well known and reliable. Therefore, Matlab was used for this research.

All operating parameters used in the polarization model can be found in Table. 1.

**Table. 1. Operating parameters used in the polarization model [27-31].**

| Parameters | Value |
|---|---|
| Operating pressure, $P$ (atm) | 1 |
| Inlet temperature, $T$ (K) | 1073 |
| Number of transfer electrons in anode and cathode, $n$ | 2,4 |
| Charge transfer coefficient range, $a$ | 0.5 |
| Anode thicknesses $\delta_a$ ($\mu m$) | 500,500 |
| Cathode thicknesses $\delta_c$ ($\mu m$) | 50,30 |
| Electrolyte thicknesses $\delta_e$ ($\mu m$) | 50,25 |
| Current density ranges, $j$ ($A/m^2$) | 0-8000,0-20000 |
| Limiting Current densities, $j_L$ ($A/m^2$) | 7500,19500 |
| Anode exchange current density, $j_{0a}$ ($A/m^2$) | 5300 |
| Cathode exchange current density, $j_{0c}$ ($A/m^2$) | 2000 |
| Leakage current density ranges, $j_{Leak}$ ($A/m^2$) | 20-100,0-20 |

## 2.1. Leakage current density

The leakage current density ($j_{Leak}$) influences the activation and concentration losses, but does not affect the ohm loss. The ohm loss is a function of the cell operating current density.

$$\eta_{act}, \eta_{conc} = f(j_{gross}), \ j_{gross} = j + j_{Leak} \tag{3}$$

Therefore:

$$\eta_{act}, \eta_{conc} = f(j_{Leak}), \ \eta_{ohm} = f(j) \tag{4}$$

Where $j$ is the operating current density and $j_{gross}$ is the sum of leakage current density and operating current density. Generally, the leakage current density is related to the electronic leakage through the electrolyte and the gas leakage due to the unsealed cell configuration [32]. Leakage current density decreases the OCV of the cell and causes it to be lower than its thermodynamic calculation's value [27].

## 2.2. Activation over-potential

The appearance of activation loss is much more frequent in low- and moderate-temperature fuel cells than in high-temperature cells. In addition, its value is higher in the cathode than in the anode. Instead of using simplified models such as the Tafel equation or the linear current-voltage relationship, which could be applied under different operating conditions, the general Butler-Volmer equation [2, 28] was chosen to calculate the corresponding anodic and cathodic voltage losses. The Butler-Volmer equation utilized in this research is as follows:

$$j = j_0 \left[ exp\left( a * n * F * {^{\eta_{act}}/_{RT}} \right) - exp\left( (1 - a) * n * F * {^{\eta_{act}}/_{RT}} \right) \right] \tag{5}$$

$$\eta_{act,i} = \frac{RT}{F} sinh^{-1} \left( {^j}/_{2 * j_{0,i}} \right), \ i = a, c \tag{6}$$

These formulas would ultimately provide solutions for $j$ and $\eta_{act}$. $j_0$ (A/m²) stands for exchange current density, $a$ is charge transfer coefficient, $n$ is the number of electrons in transfer, $F$ is the Faraday constant (C/mol), $R$ is the universal gas constant (J/mol-K), $T$ (K) is the temperature

of the cell, and $i$ stands for anode and cathode. The $j_0$ is the most effective factor when losses occur.

The higher $j_0$, the more active an electrode would be. Since $a$ is responsible for a partial change in the voltage loss and causes the reaction rate constant to change, it is commonly given a value of 0.5 [28]. Hence, the activation losses are defined for this model as:

$$\eta_{act,a} = \frac{RT}{F} * ln\left[ j\Big/2 * j_{0,a} + \sqrt{\left(j\Big/2 * j_{0,a}\right)^2 + 1} \right] \tag{7}$$

$$\eta_{act,c} = \frac{RT}{F} * ln\left[ j\Big/2 * j_{0,c} + \sqrt{\left(j\Big/2 * j_{0,c}\right)^2 + 1} \right] \tag{8}$$

$j_o$ is a function of temperature and is known to be related to the charge transfer resistance ($r_{ct}$) $\Omega$ m$^2$ as follows [27],

$$r_{ct} = RT \:/\: nFj_0 \tag{9}$$

$$j_0 = RT \:/\: nFr_{ct} \tag{10}$$

Reducing the activation loss is very important and there are some methods to do it; for example, increasing the operating temperature of fuel cell results in the increase of $j_0$; increasing the electrode surface, which increases the effective level of nominal electrode surface (length and width), increases $j_0$; as well as, increasing the density of reactants, and finally increasing pressure [27].

Activation over-potential exists at both anode and cathode. Nevertheless, whereas the $j_o$ at this fuel cell is very high, the activation loss is not that considerable. Because of greater exchange current density in the anode than in the cathode, this kind of over-potential is much higher at the cathode. Figures 1a and 1b show the results of the proposed model for activation loss, considering leakage current density of 20 and 100 A/m$^2$ in both anode and cathode, respectively.
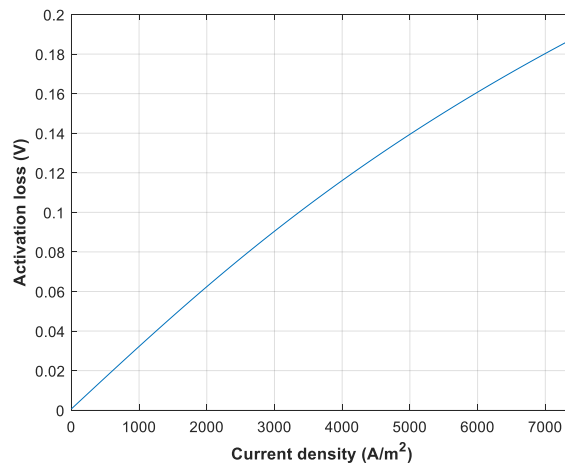


Fig. 1a: Activation loss as a function of current density considering a leakage current density of 20 A/m$^2$.
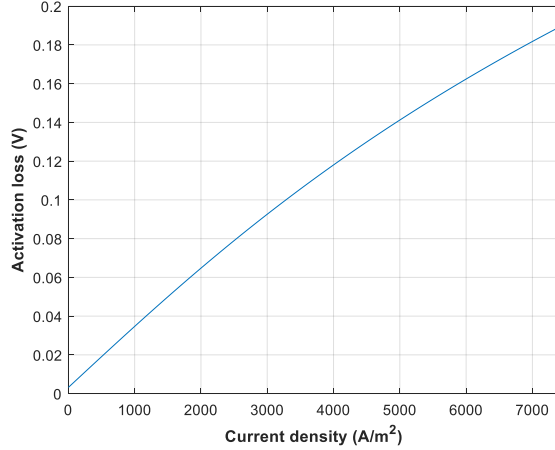
Fig. 1b: Activation loss as a function of current density considering leakage current density of 100 A/m$^2$.

## 2.3. Ohmic over-potential

Ohmic loss in which electrolyte and the electrodes of the fuel cell are involved, takes place as result from the resistance to the flow of ions in ionic conductors and the resistance to the flow of electrons in electronic conductors. Since these resistances follow the Ohm's law, the total ohmic voltage loss ($\eta_{ohm}$) would be defined as [29, 32],

$$\eta_{ohm} = R_{ohm} \, j \tag{11}$$

$$\eta_{ohm} = R_{ohm} j = (\rho_a \delta_a + \rho_c \delta_c + \rho_e \delta_e) j \tag{12}$$

Where $R_{ohm}$ is the ohmic resistance ($\Omega$), $\rho$ is resistivity of the medium ($\Omega$ m), and $\delta$ is the thickness of the medium (m); $\rho_a$, $\rho_c$, and $\rho_e$ are the electronic and ionic resistivity of the SOFCs components, respectively. $\delta_a$, $\delta_c$, and $\delta_e$ are the thicknesses of anode, cathode, and electrolyte, respectively. The electronic resistivity in the anode and the cathode as well the ionic resistivity in the electrolyte can be calculated by the following equations, valid for the materials considered above for the 3 layers [29],

$$\rho_a = 0.00008114 \exp(\frac{600}{T}) \tag{13}$$

$$\rho_c = 0.0000298 \exp(\frac{-1392}{T}) \tag{14}$$

$$\rho_e = 0.0000294 \exp(\frac{10350}{T}) \tag{15}$$

Decreasing the ohm loss is very important and there are different methods to reduce it; for example: utilizing electrodes and electrolytes with highest electronic and ionic conductance, suitable design for connection of fuel cells, and reduction of electrolyte thickness. This latter method could be problematic in some cases, since sometimes the electrolyte is regarded as the mechanical support for the electrode. Therefore, reducing its thickness decreases the mechanical strength of the cell, which will affect the circulation of current and also be an obstacle for the connection of electrodes [27].

The resistance of the fuel cell components is determined by their material specification and thicknesses. Resistance of anode and electrolyte is reduced by increasing temperature, but resistance at cathode tends to have an inverse effect. However, the resistance of both electrodes

6

in comparison with the electrolyte is negligible. Figure 2 illustrates the total ohm loss in the cell as a function of current density.
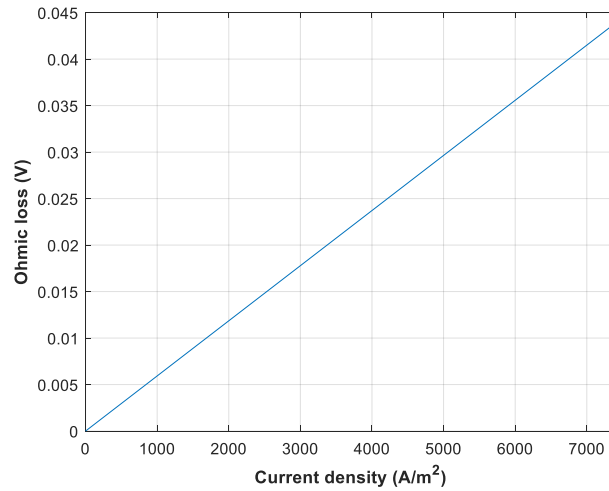


Fig. 2: Ohmic loss as a function of current density.

## 2.4. Concentration over-potential

Concentration loss represents the effects of pressure and concentration on voltage and is considerable when we have a converting system for the fuel or use air instead of oxygen. The presence of nitrogen in the cathode of the fuel cell represents a reduction in oxygen concentration and can result in issues that can increase the concentration over-potential. Under this scenario, when the cell is working, the concentration of the oxygen existing alongside the electrode would be reduced as time goes by. This oxygen concentration reduction depends on such factors as the amount of current taken from the cell, the airflow around the cathode, and the localized oxygen substitution rate. In the other side of the fuel cell, if the hydrogen is injected to the anode as time goes by, the hydrogen pressure would decrease as the hydrogen is consumed, which depends on the amount of the current taken from the cell and parameters related to the hydrogen fuel feeding system [27].

A common equation for total $\eta_{conc}$, which has been previously formulated in the literature [27, 29, 33-34] has been used for this study and is shown below,

$$\eta_{conc} = -\frac{RT}{nF} * \ln(1 - \frac{j}{j_L}) \tag{16}$$

Where $j_L$ is the limiting current density. The concentration loss is considerable, especially when the cell works at high current density and high utilization factor ranges. If the partial pressure of gases could not be tolerated by the cell, then the total voltage loss will be increased by concentration loss and consequently the cell operation will be stopped.

Ohmic and cathode activation losses are the most important over-potentials within normal operating range of SOFCs, but voltage loss, because of the cathode concentration over-potential, can also be considerable when SOFCs works near to the limiting current density. The cathode has a higher concentration loss in comparison with the anode. Whereas the exchange current density of the cathode directly influences the rate of electrochemical reaction in the cathode, the low rate of the electrochemical reaction in the cathode could cause a high cathode concentration loss at the cell [27]. Figures 3a and 3b demonstrate the results of the proposed

7

model for concentration loss, considering leakage current density of 20 and 100 A/m$^2$ in both anode and cathode, respectively.
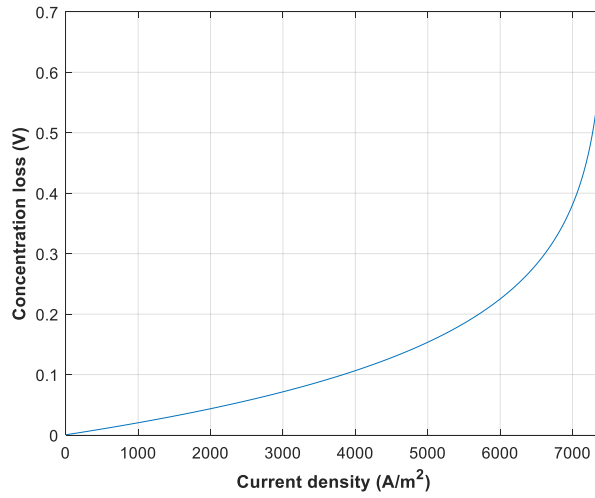


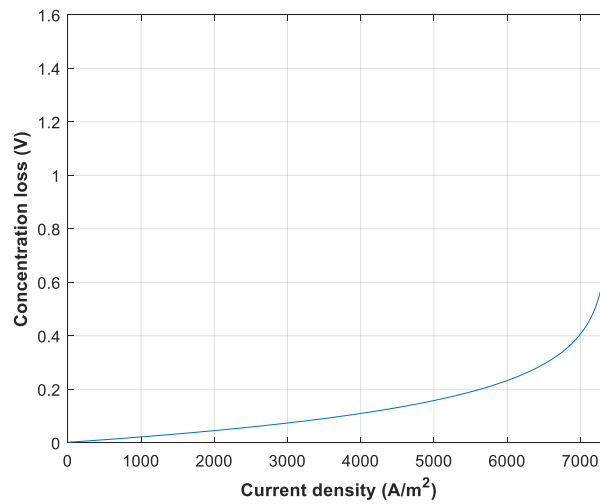Fig. 3a: Concentration loss as a function of current density considering leakage current density of 20 A/m$^2$.



Fig. 3b: Concentration loss as a function of current density considering leakage current density of 100 A/m$^2$.

## 3. Results and discussion

### 3.1. Polarization curves validation

Polarization and power density curves as a function of current density are illustrated in Figures 4a and 4b. The maximum power density for this anode-supported button cell is 3205 W/m$^2$ which was obtained at an effective cell voltage of 0.57 V, and a current density of 5620 A/m$^2$. These results showed good agreement with other modeling results [28], which are illustrated in Figure 5. The details regarding fuel and oxidant inlet condition can be found in [28].
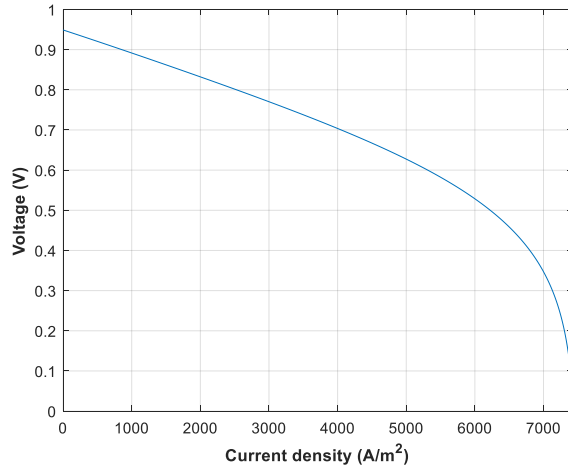
Fig. 4a: Polarization curve as a function of current density (T=1073 K, P=1 atm).
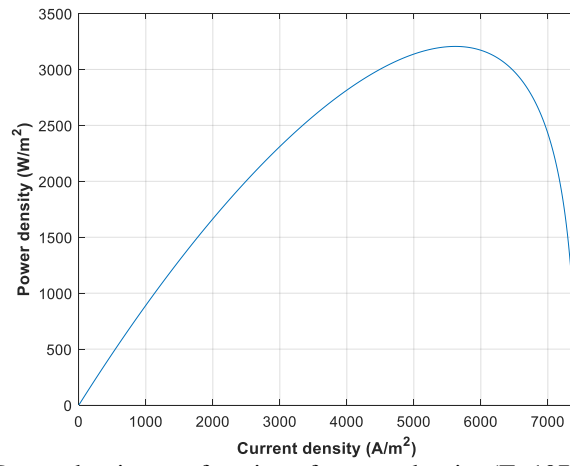


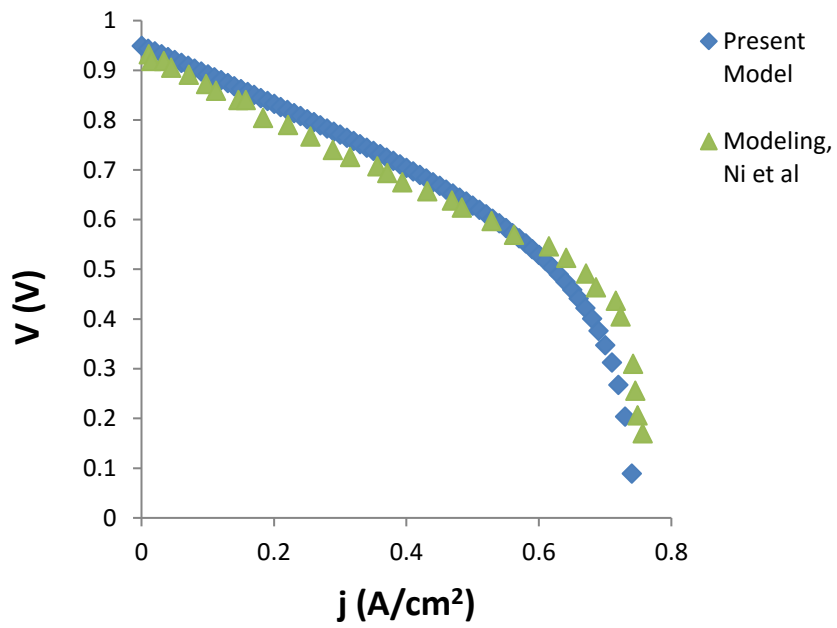Fig. 4b: Power density as a function of current density (T=1073 K, P=1 atm).



Fig. 5: Comparison of polarization curve as a function of current density for current model and the model by [28].

Also, another simulation was done by changing the thickness of the cell layers, the range of current density, and the limiting current density [30]. The results for this simulation are shown in Figures 6a and 6b. The maximum power density for this new anode-suported button cell is 8800 W/m$^2$ which was obtained at an effective cell voltage of 0.61 V, and a current density of 14200 A/m$^2$. These results showed an acceptable agreement with experimental data found in the literature [30], which is illustrated in Figure 7. The details about fuel and oxidant inlet condition can be found in [30].
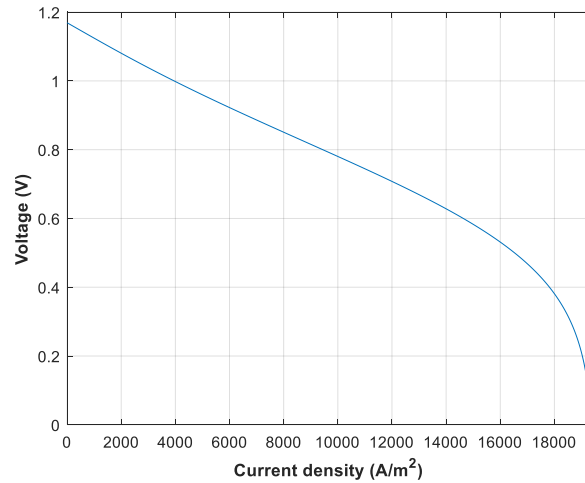


Fig. 6a: Polarization curve as a function of current density (T=1073 K, P=1 atm).



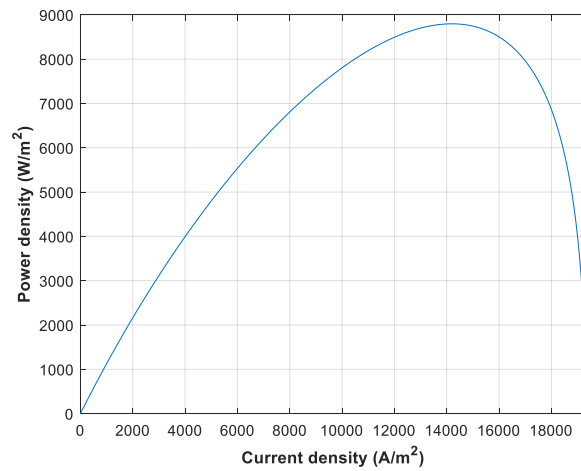Fig. 6b: Power density as a function of current density (T=1073 K, P=1 atm).
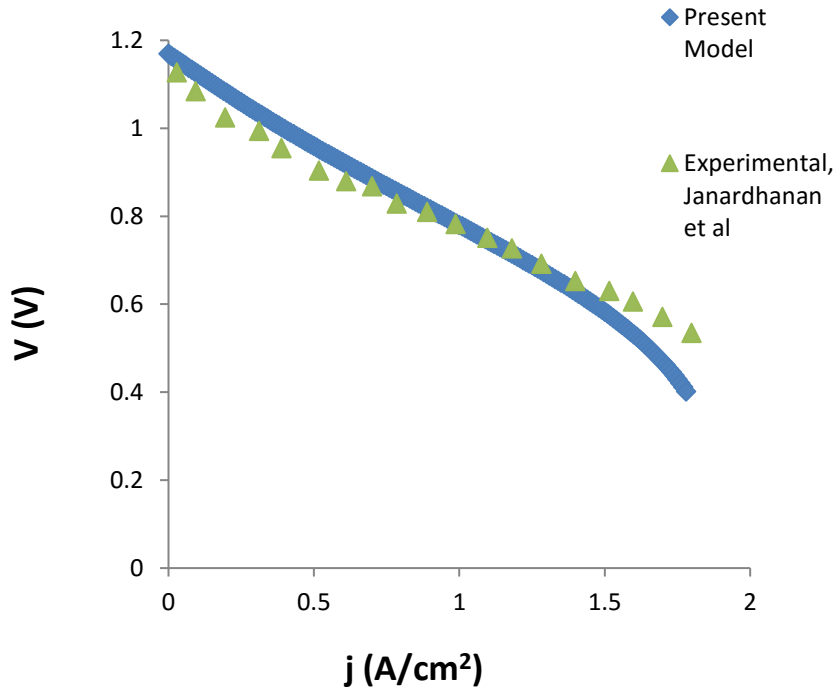
Fig. 7: Vaidation of polarization curve as a function of current density for current model and the experimental data by [30] .

A comparison between the effective results of the present study and some of the previous studies are shown in Table. 2. The quantification of the results in Table. 2 are based on the technical review of the references, which were discussed in the literature review.

**Table. 2. Comparison between the effective results of the present study and some of the previous studies.**

| Authors | Year | P (bar) | T (K) | Fuel | $U_f$ | j (A/m²) | V (Volt) | Specific Power (W/m²) | Electrical Efficiency (%) | Ref. |
|---------|------|---------|-------|------|-------|----------|----------|----------------------|--------------------------|------|
| **Present study** | - | 1 | 1073 | $CH_4$ | 0.8 | 5620 | 0.57 | 3205 | 45.8 | - |
| Riensche et al. | 1998 | NA | 1123 | NA* | 0.8 | 1700 | 0.75 | 1275 | 43 | [35] |
| Chan & Ding | 2005 | 1 | 1073 | $CH_4$ | 0.7 | NA | NA | NA | NA | [36] |
| Zhang et al. | 2005 | 1.08 | 1273 | NA | 0.85 | 1780 | 0.7 | 1250 | 52 | [37] |
| Braun et al. | 2006 | NA | 1073 | $H_2$ | 0.85 | 5700 | 0.75 | 4300 | 30.2 | [38] |
| Akkaya et al. | 2007 | 1.11 | 1203 | NA | 0.8 | 2000 | 0.72 | 1440 | NA | [39] |
| Chung et al. | 2008 | NA | 913 | $CH_4$ | 0.67 | NA | 0.7 | NA | 42.5 | [40] |
| Akkaya et al. | 2009 | 1.08 | 1273 | $CH_4$ | 0.75 | 1800 | 0.67 | 1200 | 55.4 | [41] |

| Su et al. | 2016 | 1.01 | 1073 | $H_2$ | 0.8 | 7713 | NA | NA | NA | [21] |

*: Not Available

### 3.2. Investigating a number of effective parameters on the polarization model

### 3.2.1. Effect of the anode and cathode exchange current densities on polarization curve

The effect of anode exchange current density was shown in Figure 8a; the higher exchange current density in the anode leads to decreased in loss and increased performance in the cell. Also in Figure 8b it is shown that increasing the exchange current density in the cathode results in an increased performance, but considering its value, it has a lower effect on the cell performance in comparison with changes in the anode.
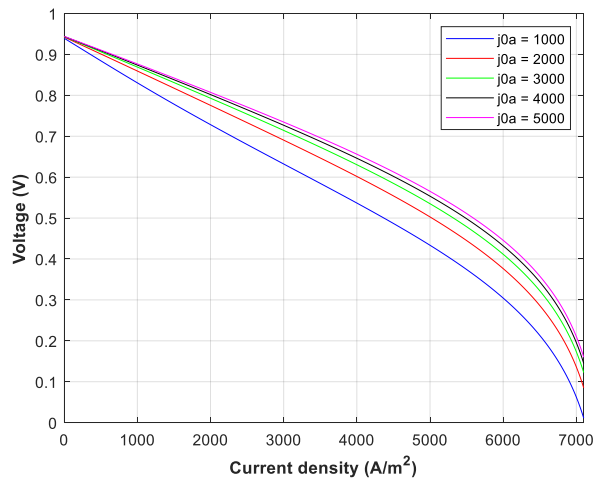


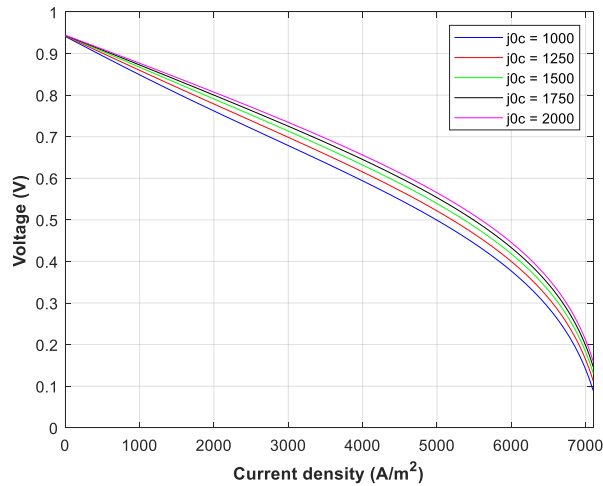Fig. 8a: Effect of $j_{0a}$ on polarization curve.



Fig. 8b: Effect of $j_{0c}$ on polarization curve.

### 3.2.2. Effect of leakage current density on polarization curve

The effect of leakage current density on the cell performance is shown in Figure 9. The decreasing trend in cell efficiency in the case of a higher leakage current density was found to be about 1% effective on diminishing the cell performance. The leakage current density is

obtained from the non-electrochemical reactions taking place at the two sides of the cell, which do not increase the operating current density.
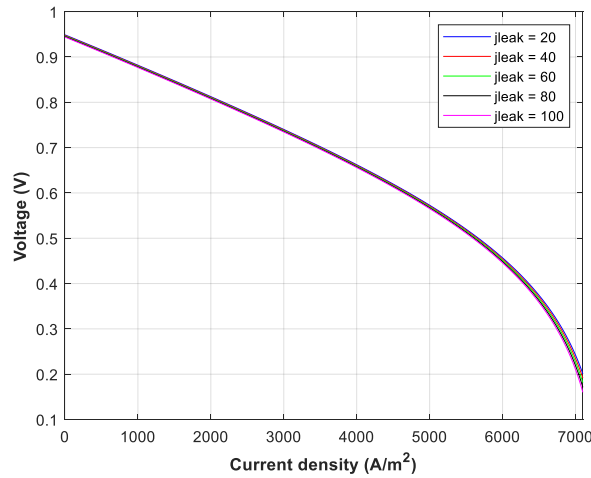


Fig. 9: Effect of $j_{Leak}$ on polarization curve.

### 3.2.3. Effect of operating temperature on polarization curve

Increasing the operating temperature of the cell resulted in a remarkable decrease on the cathode activation and electrolyte ohmic losses. This comes from the increase of both the exchange current density at the cathode and the ionic conductivity in the electrolyte, causing the improvement of the performance of SOFCs. Figure 10 clearly shows this enhanced efficiency at higher temperatures, which proves that the SOFCs performance is heavily influenced by the cell temperature.
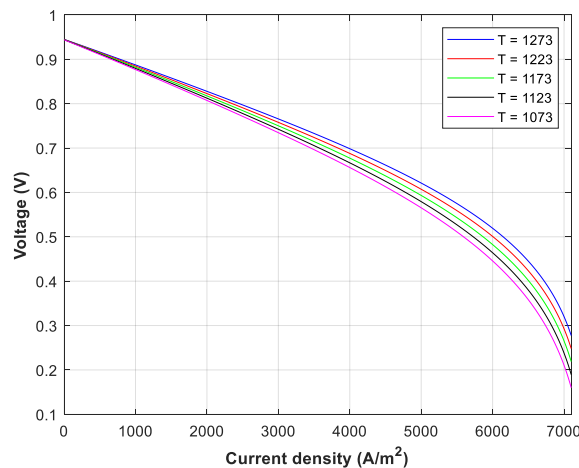


Fig. 10: Effect of temperature on polarization curve.

### 4. Conclusion

Generating a polarization model of an anode-supported SOFCs was the main objective of this research. To achieve this goal, a zero dimension polarization model was developed and then the accuracy of this own-built model was verified by performing an optimization process using a constrained non-linear multivariable function. In the polarization model of the base study, the three optimum outputs were an effective cell voltage of 0.57 V, a current density of 5620 $A/m^2$, and a power density of 3205 $W/m^2$. Then, the model was sucesfully tested against another modeling approach and also against experimental data found in the literature within a low and a high range of current densities. The results obtained herein are encouraging as the

modeling approach developed here has the merit of being not excessively computer time consuming, but robust and reliable at the same time. Furthermore, a parametric analysis was carried out to point out which parameters have a significant influence on the overall cell performance. In particular, the following parameters were accounted for this analytical study: $j_{0a}$, $j_{0c}$, $j_{Leak}$, and T.

## Nomenclature:

| | |
|---|---|
| $V_{cell}$ | Cell effective voltage, V |
| $E_{cell}$ | Cell equilibrium voltage, V |
| $j_0$ | Exchange current density, A m$^{-2}$ |
| $a$ | Charge transfer coefficient |
| $j_{Leak}$ | Leakage current density, A m$^{-2}$ |
| $j$ | Current density, A m$^{-2}$ |
| $j_L$ | Limiting current density, A m$^{-2}$ |
| $r_{ct}$ | Charge transfer resistance, $\Omega$ m$^2$ |
| $R_{ohm}$ | Ohmic resistance, $\Omega$ |
| $\rho$ | Resistivity, $\Omega$ m |
| $\delta$ | Thickness, m |
| $\eta_{act}$ | Activation loss, V |
| $\eta_{ohm}$ | Ohmic loss, V |
| $\eta_{Conc}$ | Concentration loss, V |
| $V_{Leak}$ | Leakage loss, V |
| $j_{gross}$ | Sum of leakage current density and operating current |
| $j_{0a}$ | density, A m$^{-2}$ |
| $j_{0c}$ | Anode exchange current density, A m$^{-2}$ |
| $N$ | Cathode exchange current density A m$^{-2}$ |
| $P$ | Number of transfere electrons in anode and cathode |
| $T$ | Operating pressure, Pa |
| $F$ | Inlet temperature, K |
| $R$ | Faraday Constant, C mol$^{-1}$ |
| | Gas constant, J mol$^{-1}$K$^{-1}$ |

## References

[1] Chan S.H., Ding O.L., simulation of a solid oxide fuel cell power system fed by methane, International Journal of Hydrogen Energy 30 (2005), 167-179.

[2] Chan SH, Low CF, Ding OL, Exergy and energy analysis of simple solid oxide fuel systems, J Power Sources 103(2002), 188–200.

[3] Hassan Ali Ozgoli, Hossein Ghadamian, Mohammad Pazouki, Economic Analysis of Biomass Gasification-Solid Oxide Fuel Cell-Gas Turbine Hybrid Cycle, International Journal of Renewable Energy Research, 2017 (7); 1007-1018.

[4] HA Ozgoli, H Ghadamian, R Roshandel, M Moghadasi, Alternative Biomass Fuels Consideration Exergy and Power Analysis for Hybrid System Includes PSOFC and GT Integration, Energy Sources, Part A: Recovery, Utilization, and Environmental Effects, 2015 (37); 1962-1970.

[5] Hassan Ali Ozgoli, Hossein Ghadamian, Hooman Farzaneh, Energy Efficiency Improvement Analysis Considering Environmental Aspects in Regard to Biomass Gasification PSOFC/GT Power Generation System, 2013 (17); 831-841.

[6] Ghasem Arab, Hossein Ghadamian, Saeed Abbasi, Thermo-economic modeling of an atmospheric SOFC/CHP cycle: an exergy based approach, Mechanics & Industry, 2014 (15); 113-121.

[7] Ghasem Arab, Hossein Ghadamian, Thermo economic modeling and parametric analysis of a PSOFC/GT hybrid cycle, Iranian Journal of Chemistry and Chemical Engineering, 2013 (32); 93-103.

[8] H Ghadamian, AA Hamidi, H Farzaneh, HA Ozgoli, Thermo-economic analysis of absorption air cooling system for pressurized solid oxide fuel cell/gas turbine cycle, 2012 (4); 043115.

[9] Feng Zhao, Anil V. Virkar, "Dependence of polarization in anode-supported solid oxide fuel cells on various cell parameters". Journal of Power Sources 141 (2005) 79–95.

[10] Huayang Zhu, and Robert J. Kee, "Modeling Distributed Charge-Transfer Processes in SOFC Membrane Electrode Assemblies", Journal of the Electrochemical Society, 155 (7), B715-B729 (2008).

[11] Kurtis P. Recknagle∗, Emily M. Ryan, Brian J. Koeppel, Lenna A. Mahoney, Moe A. Khaleel, Modeling of electrochemistry and steam–methane reforming performance for simulating pressurized solid oxide fuel cell stacks", Journal of Power Sources 195 (2010) 6637–6644.

[12] K. Daneshvar, G. Dotelli, C. Cristiani, R. Pelosato, M. Santarelli, "Modeling and Parametric Study of a Single Solid Oxide Fuel Cell by Finite Element Method", Fuel Cells, Volume 14, Issue 2, Pages 189–199, April 2014.

[13] Hui-Chung Liu, Chien-Hsiung Lee, Yao-Hua Shiu, Ryey-Yi Lee, Wei-Mon Yan, "Performance simulation for an anode-supported SOFC using Star-CD code, Journal of Power Sources 167 (2), 406-412, 2007.

[14] Yakab.H., Ogiwara T., Hishinuma M., Yasuda I., 3-D model calculation for planar SOFC, Journal of Power Sources 102(2001), 144–154.

[15] Chan S.H., Khor K.A., Xia Z.T., A complete polarization model of a solid oxide fuel cell and its sensitivity to the change of cell component thickness, Journal of Power Sources 93(2001), 130-140.

[16] Petruzzi L., Cocchi S., Fineschi F., A global thermo-electrochemical model for SOFC systems design and engineering, Journal of Power Sources,118(2003), 93-107.

[17] Autissier N., Larrain D., Van herle J., Favrat D., Modeling and experimental validation of solid oxide fuel cell materials and stacks, J. Power Sources 131(2004), 313–319.

[18] Liangzhu Zhu, Lei Zhang, Anil V. Virkar, "A parametric model for solid oxide fuel cells based on measurements made on cell materials and components". Journal of Power Sources 291 (2015) 138-155.

[19] Shuanglin Shen, Liejin Guo, Hongtan Liu, "A polarization model for solid oxide fuel cells with a Bi-layer electrolyte", International Journal of Hydrogen Energy 41 (2016), 3646-3654.

[20] Hiroyuki Shimada, Toshio Suzuki, Toshiaki Yamaguchi, Hirofumi Sumi, Koichi Hamamoto, Yoshinobu Fujishiro, "Challenge for lowering concentration polarization in solid oxide fuel cells", Journal of Power Sources 302 (2016) 53-60.

[21] Shichuan Su, Qiang Zhang, Xiang Gao, Vijay Periasamy, Wei Kong, "Effects of changes in solid oxide fuel cell electrode thickness on ohmic and concentration polarizations", International Journal of Hydrogen Energy 41 (2016), 16181-16190.

[22] Fergus J.W., Hui R., Li X., Wilkinson D.W., Zhang J., Solid oxide fuel cells: materials properties and performance, 2008, CRC Press.

[23] Millington R.J., Quirk J.M., Permeability of porous solids, Transactions of the Faraday Society, 1961, vol. 57, pp. 1200-1207.

[24] Singhal S.C., Kendall K., High temperature solid oxide fuel cells: fundamentals, design and applications, 2003, Elsevier.

[25] K. Daneshvar, A. Fantino, G. Dotelli, C. Cristiani, R. Pelosato, M. Santarelli, "Multi-Physics Simulation of a Circular-Planar Anode-Supported Solid Oxide Fuel Cells", at COMSOL conference, Milan, Italy, October 2012.

[26] Ghadamian, H., 2003, PhD thesis "Simulation, Designing, and Developing an Optimized Fuel Cell Model Using Mathematical Programing and Exergy Analysis", Azad University (Science& Research branch), Tehran, Iran.

[27] Larminie J., Dicks A., 2000, Fuel Cell Systems Explained, John Wiley and Sons.

[28] Ni M., Leung D.Y.C., Leung M.K.H., Modeling of methane fed solid oxide fuel cells: Comparison between proton conducting electrolyte and oxygen ion conducting electrolyte, Journal of Power Sources 183 (2008) 133–142.

[29] Cali M., Santarelli M.G.L., Leone P., Design of experiments for fitting regression models on the tubular SOFC CHP 100kWe: Screening test, response surface analysis and optimization, International Journal of Hydrogen Energy 32(2007) 343-358.

[30] Janardhanan V.M., Deutschmann O., CFD analysis of a solid oxide fuel cell with internal reforming: Coupled interactions of transport, heterogeneous catalysis and electrochemical processes, Journal of Power Sources 162 (2006) 1192–1202.

[31] Xie Y., Xue X., "Multi-scale electrochemical reaction anode model for solid oxide fuel cells". Journal of Power Sources 209 (2012), 81-89.

[32] Yahya A, Ferrero D, Dhahri H, Leone P, Slimi K, Santarelli M. Electrochemical performance of solid oxide fuel cell: Experimental study and calibrated model. Energy 2018; 142:932–43.

[33] H. Mahcene, H. Ben Moussa, H. Bouguetaia, B. Bouchekima and D. Bechki, Losses Effect on Solid Oxide Fuel Cell Stack Performance, The Second International Workshop on Hydrogen. Ghardaia, Algeria, 27-29 October 2007.

[34] Sharaf, O. Z.; Orhan, M. F. 2014. "An overview of fuel cell technology: Fundamentals and applications," Renewable and Sustainable Energy Reviews, Elsevier, vol. 32(C), pages 810-853.

[35] Ernst Riensche, Ulrich Stimming, Guido Unverzagt, "Optimization of a 200 kW SOFC cogeneration power plant Part I: Variation of process parameters", Journal of Power Sources 73(1998), 251-256.

[36] S.H. Chan, O.L. Ding, "Simulation of a solid oxide fuel cell power system fed by methane", International Journal of Hydrogen Energy 30 (2005) 167-179.

[37] W. Zhang, E. Croiset, P.L. Douglas, M.W. Fowler, E. Entchev, "Simulation of a tubular solid oxide fuel cell stack using AspenPlus$^{TM}$ unit operation models", Energy Conversion and Management 46 (2005) 181–196.

[38] R.J. Braun, S.A. Klein, D.T. Reindl, "Evaluation of system configurations for solid oxide fuel cell-based micro-combined heat and power generators in residential applications", Journal of Power Sources 158 (2006) 1290–1305.

[39] Ali Volkan Akkaya, Bahri Sahin, Hasan Huseyin Erdem, "Exergetic performance coefficient analysis of a simple fuel cell system", International Journal of Hydrogen Energy 32 (2007) 4600 – 4609.

[40] Tsang-Dong Chung, Wen-Tang Hong, Yau-Pin Chyou, Dong-Di Yu, Kin-Fu Lin, Chien-Hsiung Lee, "Efficiency analyses of solid oxide fuel cell power plant systems", Applied Thermal Engineering 28 (2008) 933–941.

[41] Ali Volkan Akkaya, Bahri Sahin, Hasan Huseyin Erdem, "Thermodynamic model for exergetic performance of a tubular SOFC module", Renewable Energy 34 (2009) 1863–1870.